

Bulk Copolymerization of Dimethyl Meta-Isopropenyl Benzyl Isocyanate (TMI®): Determination of Reactivity Ratios

S. MOHAMMED, E. S. DANIELS, A. KLEIN, M. S. EL-AASSER

Emulsion Polymers Institute and Department of Chemical Engineering, Lehigh University, Bethlehem, Pennsylvania 18015

Received 30 December 1996; accepted 8 July 1997

ABSTRACT: Dimethyl meta-isopropenyl benzyl isocyanate (TMI®) is a bifunctional monomer with an unsaturation and an isocyanate group. Bulk copolymerizations of TMI with styrene, methyl methacrylate, and *n*-butyl acrylate were investigated. Polymerizations were carried out to low conversions in sealed test tubes at 70°C. The copolymer composition was determined using Fourier transform infrared (FTIR) spectroscopy. The data were analyzed using the terminal, as well as restricted penultimate, model of copolymerization. The method of Kelen–Tudos was used to calculate the reactivity ratios according to the terminal model. A nonlinear regression analysis was also carried out. Low reactivity ratio values for TMI were obtained for the copolymerizations with styrene and methyl methacrylate as a result of the inability of TMI to undergo homopolymerization. The value was higher for the copolymerization with *n*-butyl acrylate. Composition diagrams were generated, and the range of TMI concentration in the monomer charge for the preferential incorporation of TMI in the copolymer was identified. © 1998 John Wiley & Sons, Inc. *J Appl Polym Sci* **67**: 559–568, 1998

Key words: copolymerization; dimethyl meta-isopropenyl benzyl isocyanate; reactivity ratios

INTRODUCTION

Since TMI is a relatively new monomer, it was felt prudent to determine its reactivity ratios with conventional monomers, such as styrene, methyl methacrylate, and *n*-butyl acrylate. Based on the values of these reactivity ratios, a model system was chosen for preparing film-forming TMI latex terpolymers.¹ The reactivity ratios determine the composition of the copolymer in multicomponent polymerizations. It has been known for a long time² that the copolymerization behavior of monomers is quite different from their homopolymerization kinetics. As a result, the composition of a copolymer is usually different from the composi-

tion of the comonomer charge. Another interesting aspect of copolymerization is that certain monomers that are incapable of homopolymerization via free radical initiation, such as maleic anhydride and fumaronitrile, copolymerize quite easily. TMI also does not undergo radical homopolymerization due to steric factors on account of its molecular structure, which is similar to α -methyl styrene. However, TMI can be readily copolymerized with monomers such as styrene, methyl methacrylate, *n*-butyl acrylate, and ethyl acrylate.³

A variety of experimental techniques is used to determine the copolymer composition and, thereby, the reactivity ratios. The copolymer composition can be directly determined using spectroscopic techniques such as ultraviolet (UV) and Fourier transform infrared (FTIR) spectroscopy,^{4,5} on nuclear magnetic resonance (NMR).^{6,7}

Correspondence to: M. S. El-Aasser.

Journal of Applied Polymer Science, Vol. 67, 559–568 (1998)
© 1998 John Wiley & Sons, Inc. CCC 0021-8995/98/030559-10

Elemental analysis is also used.⁸ The change in the monomer charge composition can also be followed in order to yield the copolymer composition. Usually, chromatographic techniques, such as high-pressure liquid chromatography (HPLC) or gas chromatography (GC), are useful for this purpose. Once the copolymer composition is determined, the reactivity ratios can be calculated using the copolymerization equation. The popular form of the copolymerization equation is based on the first-order Markov or terminal model of copolymerization.^{9,10} This model assumes that the reactivity of a propagating polymer chain depends only on the monomer unit at the chain end. Several monomers, especially those incapable of homopolymerization, are known to deviate from the kinetic behavior predicted by the first-order Markov model. Some systems exhibit what is referred to as the second-order Markov, or penultimate behavior. In such cases, the reactivity of the propagating polymer chain depends on the penultimate monomer unit.

The penultimate effect in the copolymerization of tetrachlorocyclopropene (TCCP) with vinyl acetate and styrene was reported by Hecht and Ojha.¹¹ Although TCCP does not homopolymerize, it copolymerizes readily with several monomers. The copolymerization data indicated that TCCP did not add to a propagating polymer chain when the penultimate unit was TCCP. The reactivity ratios of vinyl acetate and styrene were determined by assuming that TCCP does not add to itself. The penultimate effect was ascribed to steric interference between the chlorine atoms of TCCP in the monomer and those in the monomer units already added to the polymer chain. Copolymerization of styrene (S) and maleic anhydride (M) has also been found to follow the penultimate model. Chen and Chang¹² observed deviations from alternating copolymerization behavior. The deviations were negative at low maleic anhydride mole fractions in the charge and positive at higher concentrations. A three-variable penultimate model (setting only $r_{MM} = 0$; r_{MM} refers to the reactivity ratio when both the penultimate and terminal units are M, i.e., maleic anhydride) was found to explain the data well.

Brown and Fujimori¹³ fitted the copolymerization data of styrene and maleic anhydride using three different forms of the penultimate model: (1) the general four-parameter model, (2) the three-parameter model ($r_{MM} = 0$), and (3) the two-parameter model ($r_{MM} = r_{SM} = 0$). The two-parameter model was determined to adequately

describe the data. The reactivity ratios were calculated using a nonlinear least-squares (NLLS) optimization routine and were found to be significantly different from those reported by Chen and Chang. Wu et al.¹⁴ investigated the alternating nature of the copolymerization of hexafluoroisobutylene and vinyl acetate using NMR. A two-parameter restricted penultimate model was determined to explain the data well. The reactivity ratios were calculated by fitting the data using this model and were found to be consistent with the ones determined from monomer sequence distributions.

In addition to the penultimate effect, deviations from the first-order Markov model could be due to depropagation during copolymerization¹⁵ or as a result of comonomer complex formation.¹⁶ Cowie et al.¹⁷ studied the copolymerization behavior of 2,4-dicyano-but-1-ene and isoprene. The data was analyzed using the terminal, penultimate, restricted three-parameter penultimate, and complex formation models. The restricted penultimate model was found to fit the experimental data best.

In this article, the bulk copolymerization of TMI (T) with styrene, methyl methacrylate, and *n*-butyl acrylate is discussed. Since TMI is incapable of homopolymerization, the data have been analyzed using the terminal as well as the restricted penultimate model (i.e., $r_{TT} = 0$).

EXPERIMENTAL

Materials

Styrene, methyl methacrylate, and *n*-butyl acrylate (all from Aldrich, Milwaukee, WI) were purified using an inhibitor removal column and stored at -2°C prior to use. TMI (Cytec, Stamford, CT), decane and dodecane (Aldrich), methanol and chloroform (spectranalyzed, Fisher, Pittsburgh, PA), and azobis(isobutyronitrile) (AIBN) (Eastman, Kingsport, TN) were used as received.

Copolymerization

Bulk radical copolymerization of TMI (T) was carried out with three different monomers: styrene (S), methyl methacrylate (MMA), and *n*-butyl acrylate (BA). The concentration of TMI in the comonomer charge was varied between 10 and 90% (w/w). The polymerizations were carried out in sealed glass test tubes using azobis(isobutyro-

nitrile) (AIBN) as the initiator at 70°C. The initiator concentration was 0.4 wt % based on the monomer. AIBN was weighed into the test tubes and dissolved in the monomer mixture. The solutions were purged with nitrogen, and the test tubes sealed. The test tubes were placed in a shaker bath maintained at 70°C. Polymerizations were carried out to low conversions (<10%) and short-stopped by immersing the tubes in an ice bath. Depending on the TMI concentration, the polymerizations were run for different periods of time in order to obtain low conversions. The conversions were determined gravimetrically.

Sample Separation

The copolymer samples were separated from the solutions in the monomer mixture by precipitating them in a nonsolvent. Decane and dodecane were used as the non-solvents, depending on the type of monomer system, as discussed in the Results and Discussion Section. The solvents were selected so as to be inert towards the NCO group of TMI. The precipitated polymers were washed several times with the non-solvent. The washed copolymer samples were dried in a vacuum oven for two days at room temperature and then for an additional five days at an elevated temperature of 70°C.

Determination of Reactivity Ratios

The copolymer composition was determined using FTIR spectroscopy. A known amount of copolymer was dissolved in chloroform, and the absorbance of the NCO peak at approximately 2260 cm⁻¹ was followed. The concentration of TMI in the copolymer was determined from an absorbance–concentration calibration curve developed earlier. The reactivity ratios were then calculated using different forms of the copolymerization equation.

RESULTS AND DISCUSSION

The Terminal Copolymerization Model

The first-order Markov or terminal model of copolymerization assumes that the reactivity of a polymer chain depends exclusively on the monomer unit at the propagating end. The copolymerization equation derived from the above assumption relates the ratio of the instantaneous rates of consumption of the two monomers (dM_1 and dM_2) with their feed concentrations (M_1 and M_2):

$$\frac{dM_1}{dM_2} = \frac{M_1 r_1 M_1 + M_2}{M_2 r_2 M_2 + M_1} \quad (1)$$

where r_1 and r_2 are the reactivity ratios of monomers 1 and 2, respectively, and are defined as

$$r_1 = \frac{k_{11}}{k_{12}} \quad (2)$$

$$r_2 = \frac{k_{22}}{k_{21}} \quad (3)$$

where k_{11} is the propagation rate constant for a polymer chain ending in M_1 adding to monomer M_1 , k_{12} is that for a polymer chain ending in M_1 adding to M_2 , and so on.

Equation (1) can be used to relate the molar ratio of monomer 1 to monomer 2 in the comonomer feed (h) to that in the copolymer (H). Fineman and Ross¹⁸ related H and h as follows:

$$G = r_1 F - r_2 \quad (4)$$

where $G = h(H - 1)/H$ and $F = h^2/H$. G is plotted against F to obtain a straight line with slope r_1 and intercept r_2 . Kelen and Tudos¹⁹ modified the above linearization method to give equal weighting to all data points. They expressed the copolymerization equation in terms of an arbitrary positive constant α .

$$\eta = \left[r_1 + \frac{r_2}{\alpha} \right] \xi - \frac{r_2}{\alpha} \quad (5)$$

where

$$\eta = \frac{G}{\alpha + F} \quad (6)$$

$$\xi = \frac{F}{\alpha + F} \quad (7)$$

When η is plotted against ξ , a straight line is obtained. Extrapolation to $\xi = 0$ and $\xi = 1$ yields $-r_2/\alpha$ and r_1 as the intercepts, where $\alpha = (F_m F_M)^{1/2}$, and F_m and F_M are the minimum and maximum F values.

A more accurate method of determining the reactivity ratios is to plot the instantaneous copolymer composition versus the comonomer charge composition over a wide charge concentration range. The reactivity ratios are then determined

Table I Copolymer Composition Data for the Radical Bulk Copolymerization of TMI (1) and Styrene (2) at 70°C

Sample	Time (min)	h_1	H_1	f_1	F_1
1	35	0.0580	0.0703	0.0548	0.0657
2	70	0.2212	0.2007	0.1811	0.1671
3	90	0.3456	0.2976	0.2568	0.2294
4	120	0.5165	0.4034	0.3406	0.2875
5	180	0.7885	0.5658	0.4409	0.3614
6	240	1.2077	0.7408	0.5470	0.4256
7	360	1.9193	0.8687	0.6575	0.4649
8	360	4.6610	1.5098	0.8234	0.6016

by fitting the experimental data with the copolymerization equation via a nonlinear method.

The experimental data discussed in the following sections were analyzed using the Kelen–Tudos technique, as well as the nonlinear method. For the latter method, the copolymerization equation was written as a function of the mole fractions of monomer 1 in the charge (f_1) and the copolymer (F_1), as follows:

$$F_1 = \frac{f_1(r_1 f_1 + 1 - f_1)}{r_2 + f_1^2(r_1 + r_2 - 2) + 2f_1(1 - r_2)} \quad (8)$$

The Penultimate Model

The copolymerization data was also analyzed using the restricted penultimate model. The penultimate model assumes that the reactivity of the propagating species is affected by the penultimate monomer unit. Each monomer is characterized by two reactivity ratios. One ratio (r_{11} or r_{22}) represents the propagating species in which the penultimate and terminal monomer units are the same, while the other ratio (r_{12} or r_{21}) represents the propagating species in which the penultimate and terminal units are different, as follows:

$$r_{11} = \frac{k_{111}}{k_{112}} \quad (9)$$

$$r_{21} = \frac{k_{211}}{k_{212}} \quad (10)$$

$$r_{22} = \frac{k_{222}}{k_{221}} \quad (11)$$

$$r_{12} = \frac{k_{122}}{k_{121}} \quad (12)$$

The copolymerization equation, taking into account the penultimate effects, is expressed as

$$H = \frac{1 + \frac{r_{21}h(r_{11} + 1)}{(r_{21}h + 1)}}{1 + \frac{r_{12}(r_{22} + h)}{h(r_{12} + h)}} \quad (13)$$

Since TMI (monomer 1) is incapable of homopolymerization, $r_{11} = 0$; and eq. (13) is reduced to

$$H = \frac{1 + \frac{r_{21}h}{(r_{21}h + 1)}}{1 + \frac{r_{12}(r_{22} + h)}{h(r_{12} + h)}} \quad (14)$$

Equation (14) was used to fit the experimental data utilizing a computer program that varies the reactivity ratios systematically until the sum of

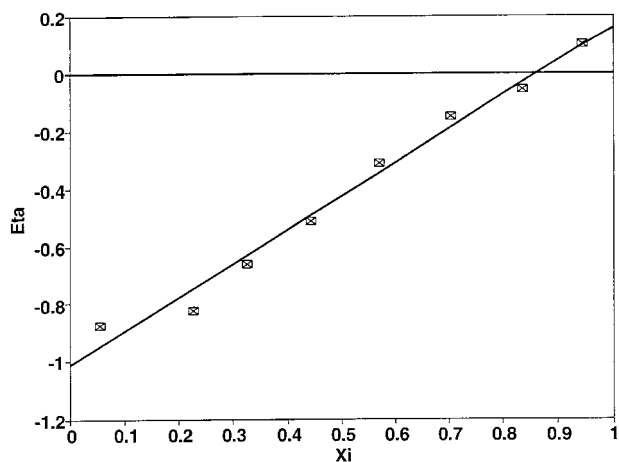


Figure 1 Kelen–Tudos plot for the copolymerization of TMI (1) and styrene (2) at 70°C.

Table II Reactivity Ratios (Terminal Model) for TMI (1) and Styrene (2) at 70°C

Method	Ratio	Value
Kelen–Tudos	r_1	0.16
Kelen–Tudos	r_2	0.84
Nonlinear	r_1	0.17
Nonlinear	r_2	0.86

the squares of the differences between the experimental and calculated values is minimized. The results for the copolymerization of TMI with S, MMA, and BA are discussed in the following sections.

Copolymerization of TMI and Styrene

Bulk copolymerization of TMI and styrene was carried out to low conversions (<10%) at different TMI concentrations, as described in the Experimental Section. Since TMI retards the polymerization kinetics, the samples with higher TMI concentration had to be polymerized for longer periods of time as shown in Table I. The molar ratios and mole fractions of TMI in the monomer charge (h_1, f_1) and the copolymer (H_1, F_1) are also shown in the table.

The copolymer samples were separated from the polymerization mixture by precipitating them in dodecane. The copolymer composition was determined using FTIR spectroscopy, as described above. The data shown in Table I were analyzed

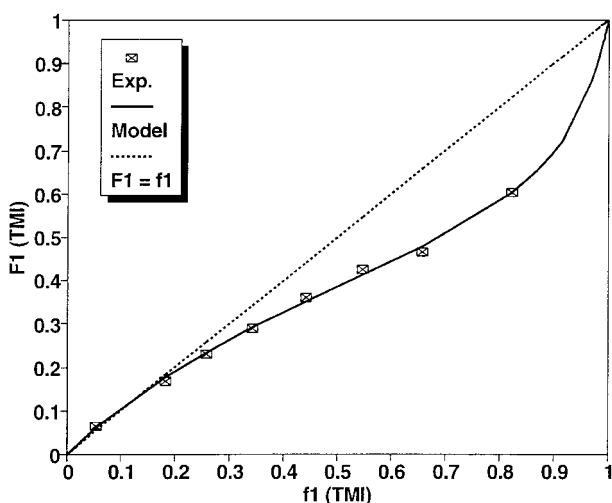


Figure 2 Copolymer composition diagram (terminal model) obtained using the nonlinear method for the copolymerization of TMI (1) and styrene (2) at 70°C.

Table III Reactivity Ratios (Penultimate Model) for TMI (1) and Styrene (2) at 70°C

Ratio	Value
r_{11}	0.00 ^a
r_{21}	0.65
r_{22}	1.12
r_{12}	1.13

^a Assumed.

using the Kelen–Tudos method and nonlinear regression. The Kelen–Tudos plot is shown in Figure 1. The reactivity ratios determined using the two methods are compared in Table II.

It can be observed from the table that there is a close match between the values of the reactivity ratios determined using the two methods. There is a large difference between the reactivity ratios of TMI and styrene, with the latter being much higher. This discrepancy could be attributed to the inability of TMI to undergo homopolymerization. The addition of styrene was favored when TMI was the terminal unit, whereas the addition of TMI was only marginally favored when styrene was the terminal unit. As a result, the addition of styrene was preferred, irrespective of the terminal unit. The copolymer composition diagram obtained via the nonlinear method is shown in Figure 2. This figure indicates that the terminal model fitted the copolymerization data very well. It can also be seen that almost all the data points

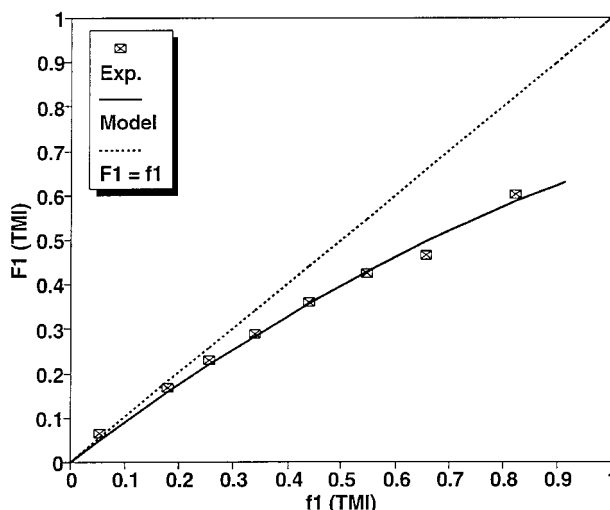


Figure 3 Copolymer composition diagram (penultimate model) for the copolymerization of TMI (1) and styrene (2) at 70°C.

Table IV Copolymer Composition Data for the Radical Bulk Copolymerization of TMI (1) and MMA (2) at 70°C

Sample	Time (min)	h_1	H	f_1	F_1
1	35	0.0558	0.1195	0.0528	0.1068
2	50	0.1248	0.2230	0.1110	0.1823
3	70	0.2137	0.3252	0.1760	0.2454
4	90	0.3332	0.4737	0.2499	0.3210
5	190	0.7466	0.5602	0.4274	0.3591
6	240	1.1441	0.7416	0.5336	0.4258
7	300	1.9727	0.8998	0.6636	0.4736
8	360	4.4289	1.2099	0.8158	0.5475

fell below the $F_1 = f_1$ line. This implies that, irrespective of the TMI concentration in the comonomer charge, the addition of styrene to the copolymer was always favored. Hence, it is difficult to incorporate TMI into a poly(TMI–styrene) copolymer. In order to determine if penultimate effects were dominant during the copolymerization, the experimental data were analyzed using the restricted penultimate model [eq. (14)]. The reactivity ratios determined using this method are collected in Table III. The copolymer composition diagram is shown in Figure 3. From the reactivity ratios, it can be deduced that when TMI was either the terminal or penultimate unit, the propagating species preferred adding onto a styrene unit. Also, when styrene constituted both the penultimate and terminal units, addition of styrene was favored over TMI. Thus, irrespective of the type of penultimate or terminal unit, addition of styrene was preferred. This result was similar to the one predicted by the terminal model. The sum of the squares of the differences between the experimental and calculated values was lower when the terminal model was used. The sum of squared deviations for the terminal model was 5.33×10^{-4} , whereas that for the penultimate model was 2.39×10^{-2} . It can therefore be concluded that the copolymerization behavior of TMI and styrene can be described well by the terminal model of copolymerization.

Copolymerization of TMI and MMA

The copolymer composition data for TMI (1) and MMA (2) are presented in Table IV. The polymerization retarding characteristics of TMI are evident from the time needed to reach approximately 5% conversion at high TMI concentrations. At the highest TMI levels, polymerizations had to be car-

ried out for 5–6 h in order to obtain even such low conversions.

Dodecane was used to precipitate the copolymer samples with low TMI content. Samples 6–8 were precipitated in decane. The samples were dried in a vacuum oven and dissolved in chloroform. FTIR spectra of the polymer solutions were taken in order to determine the copolymer composition. Reactivity ratios were determined using the Kelen–Tudos and nonlinear methods. The Kelen–Tudos plot is shown in Figure 4. The reactivity ratios obtained from the two methods were found to be quite close, as shown in Table V.

The reactivity ratio of TMI was found to be very close to zero. This indicates the lack of homopolymerization of TMI. Addition of MMA was favored when TMI was the terminal unit. However, the reactivity ratio of MMA was also determined to be much less than 1.0. This shows that addition of TMI was favored when MMA was the terminal

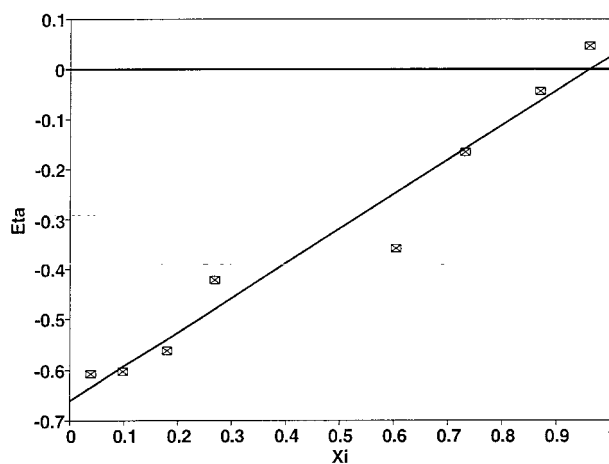


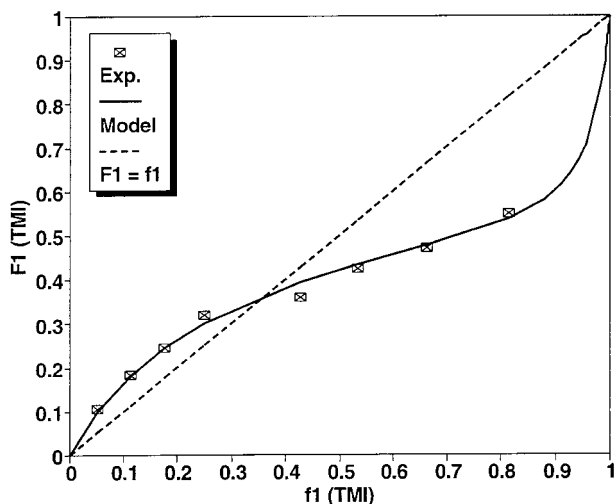
Figure 4 Kelen–Tudos plot for the copolymerization of TMI (1) and MMA (2) at 70°C.

Table V Reactivity Ratios (Terminal Model) for TMI (1) and MMA (2) at 70°C

Method	Ratio	Value
Kelen-Tudos	r_1	0.03
Kelen-Tudos	r_2	0.43
Nonlinear	r_1	0.06
Nonlinear	r_2	0.46

unit. Thus, under certain conditions, TMI is added preferentially to the growing polymer chain. This can also be seen in the copolymer composition diagram obtained via the nonlinear method (Fig. 5). In the figure, the azeotropic point where the mole fraction of TMI in the charge equals that in the copolymer is around $F_1 = f_1 = 0.35$. At this point, the copolymer composition line intersects the $F_1 = f_1$ line. It can be observed that below the azeotropic point, the experimental data lie above the $F_1 = f_1$ line. This indicates that in this concentration range ($f_1 = 0.0$ to 0.35), the amount of TMI in the copolymer is greater than that in the charge. In other words, the addition of TMI is preferred over that of MMA. Therefore, facile copolymerization of TMI and MMA is possible in this concentration range. At higher TMI concentrations, the addition of MMA is preferred; and since homopolymerization of TMI does not occur, high monomer conversions cannot be expected.

The copolymerization data were also analyzed using the restricted penultimate model [eq. (14)].

**Figure 5** Copolymer composition diagram (terminal model) obtained using the nonlinear method for the copolymerization of TMI (1) and MMA (2) at 70°C.**Table VI Reactivity Ratios (Penultimate Model) for TMI (1) and MMA (2) at 70°C**

Ratio	Value
r_{11}	0.00 ^a
r_{21}	0.18
r_{22}	0.34
r_{12}	1.04

^a Assumed.

The results are shown in Table VI and Figure 6. The reactivity ratios determined using the penultimate model indicated that when TMI was either the penultimate or the terminal unit, the propagating chain preferred adding on MMA. However, when both the penultimate and terminal units were MMA, addition of TMI was favored. Therefore, at high MMA concentrations (i.e., low f_1 values), the experimental data were above the $F_1 = f_1$ line. Both the terminal and penultimate models were found to fit the experimental data well. The former, however, had a slightly lower sum of squares of the differences between the experimental and calculated values. The sum of squared deviations for the terminal model was 1.89×10^{-3} , whereas this value was 5.82×10^{-3} for the penultimate model. The terminal model is favored in this case as it correlates the data with two adjustable parameters, as compared to the penultimate model that utilizes four parameters.

Copolymerization of TMI and BA

The final objective of using TMI was to develop room-temperature curable latexes. In order to

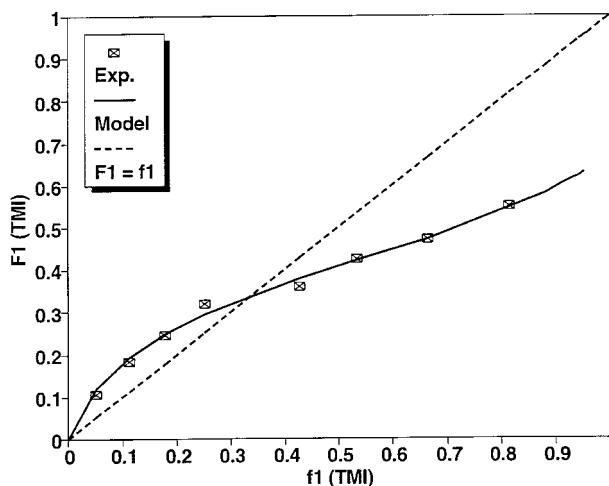
**Figure 6** Copolymer composition diagram (penultimate model) for the copolymerization of TMI (1) and MMA (2) at 70°C.

Table VII Copolymer Composition Data for the Radical Bulk Copolymerization of TMI (1) and BA (2) at 70°C

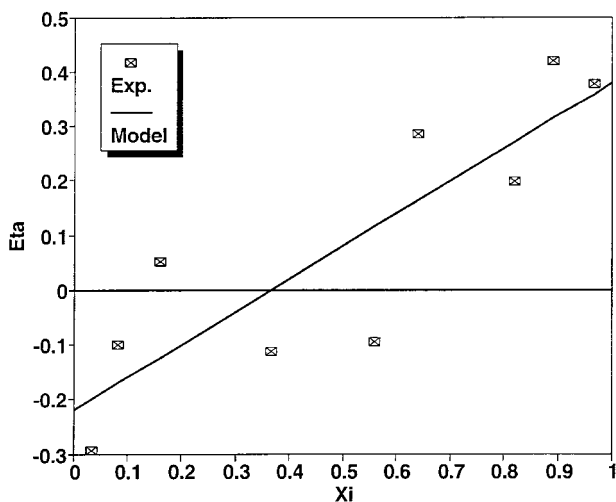
Sample	Time (min)	h_1	H_1	f_1	F_1
1	35	0.0558	0.1195	0.0661	0.2833
2	50	0.1248	0.2230	0.1373	0.4451
3	70	0.2137	0.3252	0.2144	0.5214
4	90	0.3332	0.4737	0.2980	0.4650
5	120	0.7466	0.5602	0.3891	0.4715
6	180	1.1441	0.7416	0.4886	0.5878
7	240	1.9727	0.8998	0.5977	0.5766
8	300	4.4289	1.2099	0.7181	0.6873
9	360	4.4289	1.2099	0.8514	0.7640

control the T_g of the polymer, BA was used as the elastomeric component. Therefore, the reactivity ratios of TMI and BA were also determined. Copolymerization of TMI and BA was carried out at various TMI-to-BA ratios. Polymerizations were stopped at low conversions in order to be within the applicable range of the copolymerization equation. The composition of TMI in the charge and the copolymer are shown in Table VII.

It was difficult to precipitate the copolymer as the polymerization mixture was found to be soluble in most reagents. This could be due to the low molecular weight of the copolymer. A loose precipitate was obtained when methanol was used as the nonsolvent. However, the copolymer samples crosslinked in the presence of methanol during the drying stage. Finally, decane was found to be the most suitable non-solvent for sepa-

rating the copolymer. When the polymerization mixture was poured in an excess of decane, a turbid suspension was obtained, which was found to settle and eventually dissolve in the solvent. Small amounts of the copolymer could be separated by removing the supernatant solution before all the polymer could dissolve in the solvent. The supernatant was replaced with pure decane, and the process was repeated until a sufficient amount of the copolymer sample could be separated. The sample was then washed several times with decane and dried in a vacuum oven, as described in the Experimental Section. The copolymer composition was then determined using FTIR spectroscopy. The data were analyzed using the Kelen–Tudos and the nonlinear techniques. The Kelen–Tudos plot is shown in Figure 7. The reactivity ratios determined using the two methods are compared in Table VIII.

The reactivity ratios obtained from the two methods were quite close. Unlike the copolymerization of TMI with styrene and MMA, the reactivity ratio of TMI was higher than that of the BA comonomer. The values of the two reactivity ratios indicate that the addition of TMI is preferred when BA is the terminal unit, and the addition of BA is preferred when the terminal unit is TMI.

**Figure 7** Kelen–Tudos plot for the copolymerization of TMI (1) and BA (2) at 70°C.**Table VIII Reactivity Ratios (Terminal Model) for TMI (1) and BA (2) at 70°C**

Method	Ratio	Value
Kelen–Tudos	r_1	0.38
Kelen–Tudos	r_2	0.08
Nonlinear	r_1	0.40
Nonlinear	r_2	0.08

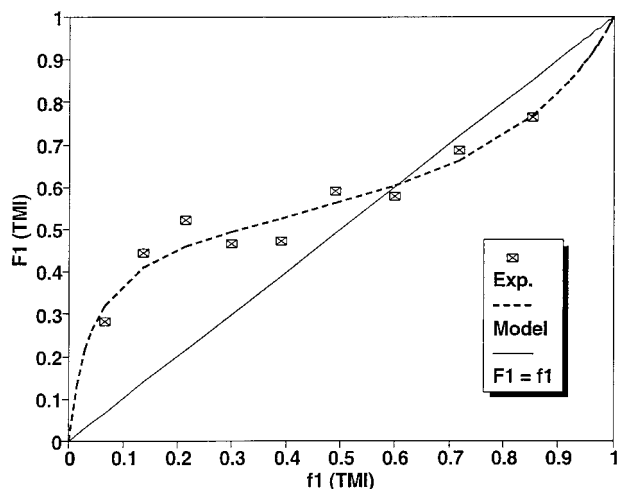


Figure 8 Copolymer composition diagram (terminal model) determined using the nonlinear method for the copolymerization of TMI (1) and BA (2) at 70°C.

However, the degree of preference in the former case was higher. Therefore, most of the data fell above the $F_1 = f_1$ line (Fig. 8). The azeotropic point where the copolymer composition equals that in the comonomer charge was found to be around $f_1 = 0.60$. At lower TMI concentrations, the amount of TMI in the copolymer was greater than that in the comonomer charge. Thus, the copolymerization of TMI with BA provides a larger window for obtaining high conversions. The results obtained by applying the penultimate model are shown in Table IX and Figure 9. The penultimate model did not fit the experimental data well and was therefore inapplicable for the TMI/BA system. This can also be seen from the unusually high value for the r_{21} reactivity ratio. According to this value, the addition of TMI is highly favored when BA is the penultimate unit and TMI is the terminal unit. This is highly unlikely as TMI does not homopolymerize. Therefore, it can be concluded that the terminal model

Table IX Reactivity Ratios (Penultimate Model) for TMI (1) and BA (2) at 70°C

Ratio	Value
r_{11}	0.00 ^a
r_{21}	3.03
r_{22}	0.11
r_{12}	0.20

^a Assumed.

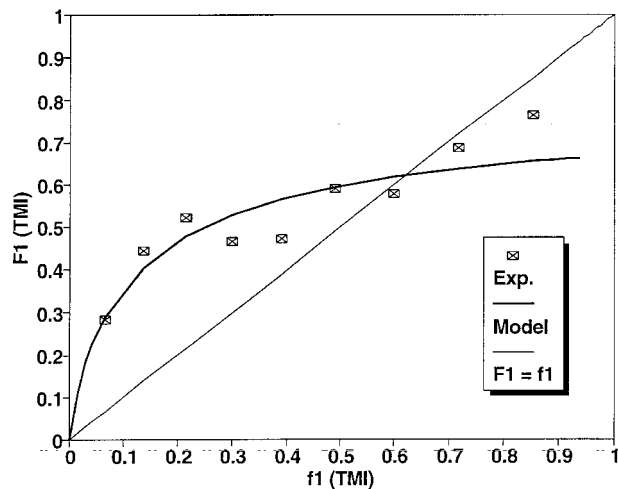


Figure 9 Copolymer composition diagram (penultimate model) for the copolymerization of TMI (1) and BA (2) at 70°C.

describes the copolymerization behavior of TMI and BA better.

CONCLUSIONS

The bulk radical copolymerization of TMI with S, MMA, and BA was investigated. The copolymerization data were analyzed using the terminal as well as the penultimate models. For the former case, the Kelen–Tudos and a nonlinear regression technique were employed in order to determine the reactivity ratios. The terminal model was found to fit the data better than the penultimate model in all three cases. The penultimate model fitted the data reasonably well for the copolymerizations with MMA and S. However, a least-squares analysis indicated that the terminal model explained the data better. The penultimate model could not be applied to the copolymerization of TMI and BA. The ease of addition of TMI to the copolymer was found to be in the order BA > MMA > S. In the copolymerization of TMI and styrene, almost all the experimental data points were found to lie below the $F_1 = f_1$ line. The composition diagrams for the copolymerizations with MMA and BA indicated azeotropic points at $F_1 = f_1 = 0.35$ and 0.60 , respectively. At this point, the composition of the copolymer was the same as that of the comonomer charge. The reactivity ratios determined in this study were found to be significantly different from those reported earlier.³ This could be attributed to the much higher

polymerization temperature used in the latter investigation.

REFERENCES

1. S. Mohammed, E. S. Daniels, A. Klein, and M. S. El-Aasser, *J. Appl. Polym. Sci.*, **61**, 911 (1996).
2. H. Staudinger and J. Schneiders, *Ann. Chim. (Paris)*, **541**, 151 (1939).
3. R. W. Dexter, R. Saxon, and D. E. Fiori, *J. Coatings Tech.*, **58**, 43 (1985).
4. G. K. Kostov and Al. T. Nikolov, *J. Appl. Polym. Sci.*, **55**, 1529 (1995).
5. S. Soundararajan, B. S. R. Reddy, and S. Rajadurai, *Polymer*, **31**, 366 (1990).
6. A. S. Brar Sunita, and C. V. V. Satyanarayana, *Polym. J.*, **24**, 879 (1992).
7. A. Rossi, J. Zhang, and G. Odian, *Macromolecules*, **29**, 2331 (1996).
8. Y. Liu, R. Mao, M. B. Huglin, and P. A. Holmes, *Polymer*, **37**, 1437 (1996).
9. T. Alfrey Jr. and G. Goldfinger, *J. Chem. Phys.*, **12**, 115 (1944).
10. F. R. Mayo and F. M. Lewis, *J. Am. Chem. Soc.*, **66**, 1594 (1944).
11. J. K. Hecht and N. D. Ojha, *Macromolecules*, **2**, 94 (1969).
12. S-A. Chen and G-Y. Chang, *Makromol. Chem.*, **187**, 1597 (1986).
13. A. S. Brown and K. Fujimori, *Makromol. Chem.*, **188**, 2177 (1987).
14. C. Wu, R. Brambilla, and J. T. Yardley, *Macromolecules*, **23**, 997 (1990).
15. G. G. Lowry, *J. Polym. Sci.*, **42**, 463 (1960).
16. J. A. Seiner and M. Litt, *Macromolecules*, **4**, 308 (1971).
17. J. M. G. Cowie, S. H. Cree, and R. Ferguson, *J. Polym. Sci., Polym. Chem. Ed.*, **28**, 515 (1990).
18. M. Fineman and S. D. Ross, *J. Polym. Sci.*, **5**, 259 (1950).
19. T. Kelen and F. Tudos, *J. Macromol. Sci., Chem.*, **A9**, 1 (1975).